AD-A041 144 EG AND G INC SALEM MASS ELECTRONIC COMPONENTS DIV F/G 9/1
REPETITIVE SERIES INTERRUPTER II.(U)
MAY 77 R SIMON, D V TURNQUIST
UNCLASSIFIED ECOM-76-1301-3 DAAB07-76-C-1301
NL

| OF |
AD
A041144

END

DATE
FILMED
8-77

Research and Development Technical Report

ECOM -76-1301-3

REPETITIVE SERIES INTERRUPTER II

Robert Simon
David V. Turnquist
EG&G Inc.
Electronic Components Division
Salem, Massachusetts 01970

May 1977

Third Triannual Report for the Period 1 January 1977 to 28 February 1977

DISTRIBUTION STATEMENT
Approved for public release:
distribution unlimited

Prepared for:

ECOM

US ARMY ELECTRONICS COMMAND FORT MONMOUTH, NEW JERSEY 07703

NOTICES

Disclaimers

The findings in this report are not to be construed as an official Department of the Army position, unless so designated by other authorized documents.

The citation of trade names and names of manufacturers in this report is not to be construed as official Government indorsement or approval of commercial products or services referenced herein.

Disposition

Destroy this report when it is no longer needed. Do not return it to the originator.

UNCLASSIFIED

SECURITY CLASSIFICATION OF THIS PAGE *(When Data Entered)*

REPORT DOCUMENTATION PAGE

READ INSTRUCTIONS BEFORE COMPLETING FORM

1. REPORT NUMBER: ECOM-76-1301-3	2. GOVT ACCESSION NO.
3. RECIPIENT'S CATALOG NUMBER	
4. TITLE *(and Subtitle)*: Repetitive Series Interrupter II.	5. TYPE OF REPORT & PERIOD COVERED: Third Triannual Report, no. 3, 1 Jan 77 to 28 Feb 77.
	6. PERFORMING ORG. REPORT NUMBER
7. AUTHOR(s): Robert Simon, David V. Turnquist	8. CONTRACT OR GRANT NUMBER(s): DAAB07-76-C-1301
9. PERFORMING ORGANIZATION NAME AND ADDRESS: EG&G Inc., 35 Congress Street, Salem, Massachusetts 01970	10. PROGRAM ELEMENT, PROJECT, TASK AREA & WORK UNIT NUMBERS: 62705 1L762705.AH.94.E1.01
11. CONTROLLING OFFICE NAME AND ADDRESS: US Army Electronics Command, ATTN: DRSEL-TL-BG, Fort Monmouth, NJ 07703	12. REPORT DATE: May 1977
	13. NUMBER OF PAGES: 39
14. MONITORING AGENCY NAME & ADDRESS *(if different from Controlling Office)*: E1	15. SECURITY CLASS. *(of this report)*: Unclassified
38 p.	15a. DECLASSIFICATION/DOWNGRADING SCHEDULE

16. DISTRIBUTION STATEMENT *(of this Report)*

Approved for Public Release; Distribution Unlimited

17. DISTRIBUTION STATEMENT *(of the abstract entered in Block 20, if different from Report)*

18. SUPPLEMENTARY NOTES

19. KEY WORDS *(Continue on reverse side if necessary and identify by block number)*

Series Interrupter
Gas Filled Device
Fuse
Thyratron
Magnetic Interaction Region

20. ABSTRACT *(Continue on reverse side if necessary and identify by block number)*

This report describes work performed from 1 Jan 77 through 28 Feb 77 on the Repetitive Series Interrupter, a hydrogen thyratron modified for opening switch operation. A description is given of two tubes designed for optical study of current interruption, and of results obtained from them. Experimental modifications are discussed and new designs for experimental interrupters are outlined.

DD FORM 1 JAN 73 1473 EDITION OF 1 NOV 65 IS OBSOLETE

UNCLASSIFIED

SECURITY CLASSIFICATION OF THIS PAGE *(When Data Entered)*

ABBREVIATIONS AND SYMBOLS

Bq	Magnetic field (kilogauss) required for quenching fault current
Ebb	Main supply voltage for tube under test
Ef	TUT cathode heater filament voltage
ξj	Magnetic field energy for RSI tube volume
Em	Magnet supply voltage
epy	Instantaneous full voltage across tube under test
Eres	TUT hydrogen reservoir voltage
Eq	Magnet circuit voltage required for quenching fault current
etd	TUT voltage drop during normal pulse operation
ib	Peak RSI-carried current
iRSI	RSI-carried current, as a function of time
L	Length of interaction tube used during test
m	Empirical exponent of proportionality between Bq and 1/L
MCCD	Magnetic-Controlled Charging Diode
N	Number of turns in magnet coil
P	TUT pressure
prr	TUT pulse repetition rate
r	Radius of interaction tube
Rcct	Resistance of magnetic field probe circuit
Rchoke	Resistance of magnetic field probe circuit integrating inductor
Rm	Magnet circuit load resistance
Rl	Pulse-forming network load resistance
Rrc	Fault network load resistance
τD	Time delay between TUT fire and magnet fire
TUT	Tube under test
β	Empirical exponent of proportionality between Bq and Ebb
δ	Empirical exponent of proportionality between Bq and ib
Δtad	Full range of deviation of delay time drift for tube fire

TABLE OF CONTENTS

LIST OF FIGURES

1. INTRODUCTION

1.1 FOREWORD

This report documents work performed from 1 January 1977 through 28 February 1977 under USAECOM Contract DAAB07-C-1301, entitled "Repetitive Series Interrupter II." This is the Third Triannual Report under the above contract. Work described herein was performed by EG&G, Inc., 35 Congress Street, Salem, Massachusetts.

1.2 BACKGROUND

Previous work has shown that Repetitive Series Interrupter (RSI) tubes are capable of reliably interrupting high voltage fault discharges, while retaining the ability to operate under normal pulse conditions. The main problem confronting this program is to assure that the RSI tubes operate stably and consistently with minimum voltage drop, and yet retain the ability to interrupt current faults with minimum additional energy requirements.

Toward this end, present work is aimed at (1) resolving the physical mechanisms of current interruption in the RSI tubes, and (2) making use of this information in the design of improved tubes. Two RSI tubes with transparent magnetic interaction regions have been constructed for optical investigations of the discharge column.

1.3 GENERAL RESULTS

Our present studies confirmed that displacement of the plasma column, by the influence of the quenching field, occurred in the expected manner. Optical studies showed a lateral displacement of the plasma light intensity during quenching, as well as a considerable increase in emission of light at the wavelengths of sodium and oxygen (major interaction wall constituents). The conclusion inferred is that narrowing of the discharge path and plasma-wall interactions are the most likely formal mechanisms for current interruption.

In addition, the potential use of a magnetic "plasma chute" (nonuniform internal diameter interaction channel) quenching tube design was also confirmed as an extremely valid design approach.

1.4 EXPERIMENTAL PROCEDURES

Test procedures and circuitry remain, for the most part, unchanged from those detailed in previous reports. Electrical measurements are made as in previous reports; optical measurements are described in Section 2. The test circuit is shown in Figure 1.

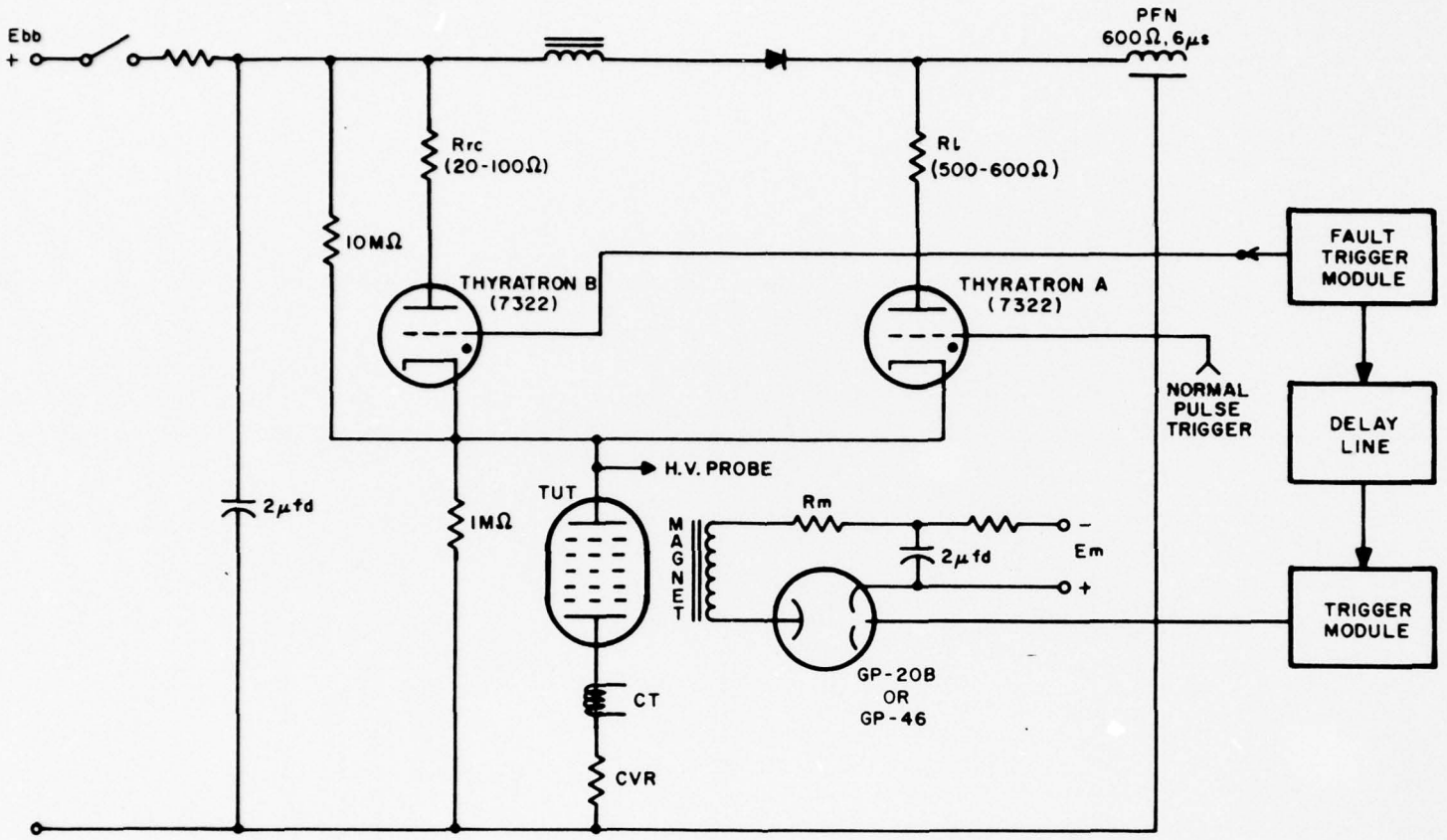

Figure 1. RSI Test Circuit.

2. CURRENT PROGRESS

2.1 TUBES UNDER STUDY

Tubes RSI 004 and RSI 005 were of primary interest during this period. Cross sections of these tubes are shown in Figures 2 and 3, and design specifications are given in Table 1.

Both tubes have a pyrex interaction column composition for optical observations. RSI 004 is a straight length of unhindered interaction column, while RSI 005 is composed of a 1-inch internal diameter tube inside of which are alternating ceramic washers and rings of 0.13 and 0.80 I.D.'s, respectively. The purpose for this design is to provide a long discharge path for the plasma column during current interruption. It was expected that the plasma discharge would be compelled, by the perpendicular magnetic field, to enter the washer-to-washer gaps, and, by reason of the longer plasma-wall interaction length, be interruptible with a lower magnetic field.

Tube pressure, for both tubes, was observed to have a slightly weaker than normal response to changes in the reservoir voltage. Pressure versus Eres ranging was performed during the gas-filling operation and reservoir inconsistency was observed until a second or third gas-filling was undertaken. Consequently, calculated pressure values for the tubes during operation must be considered potentially unreliable, even though the tubes behaved normally during testing. A possible contributing cause of this behavior may be tube bake-out at 350°C, instead of at the normal 400°C (to protect the glass seals).

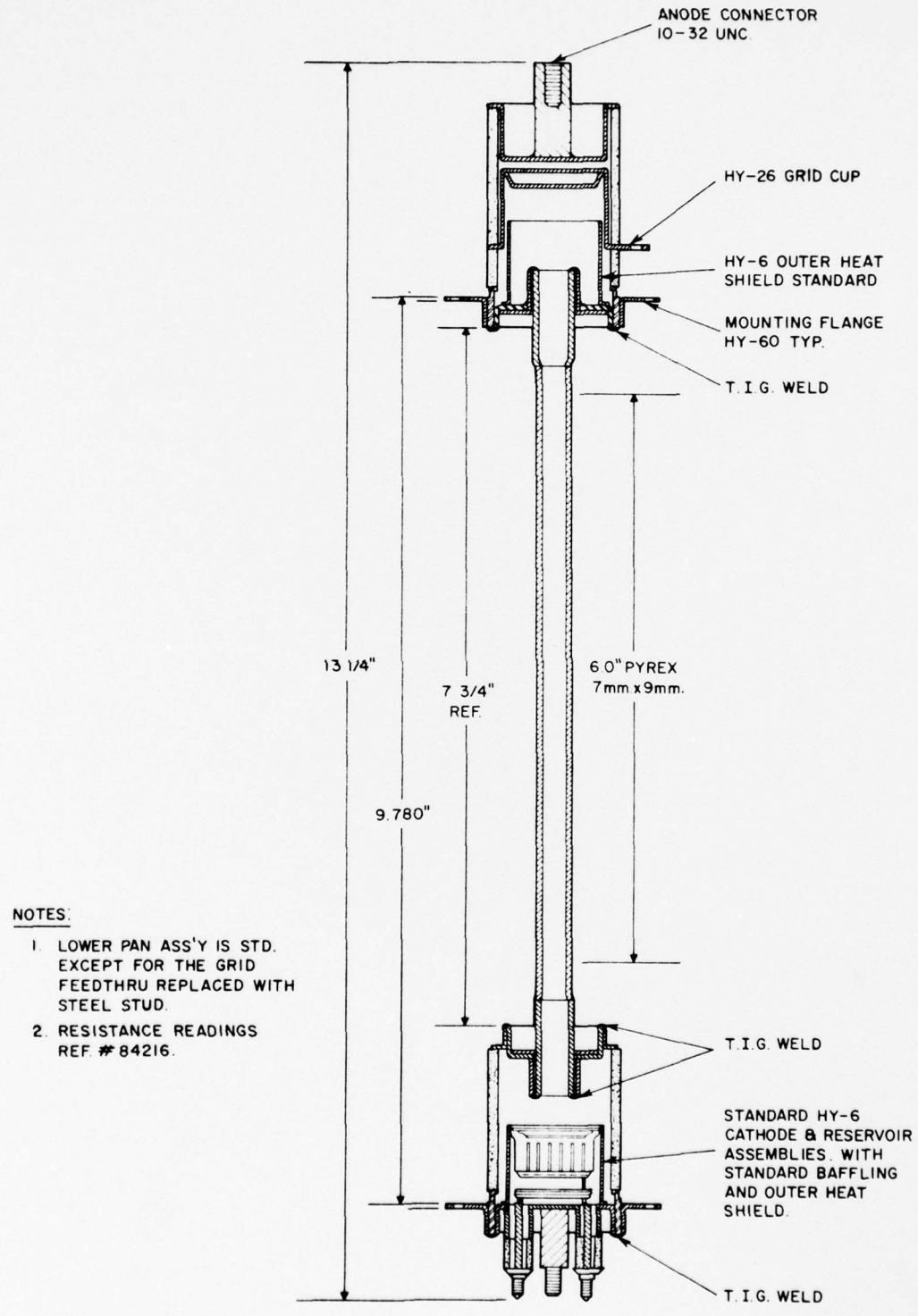

NOTES:

1. LOWER PAN ASS'Y IS STD. EXCEPT FOR THE GRID FEEDTHRU REPLACED WITH STEEL STUD.
2. RESISTANCE READINGS REF. # 84216.

Figure 2. Tube RSI 004.

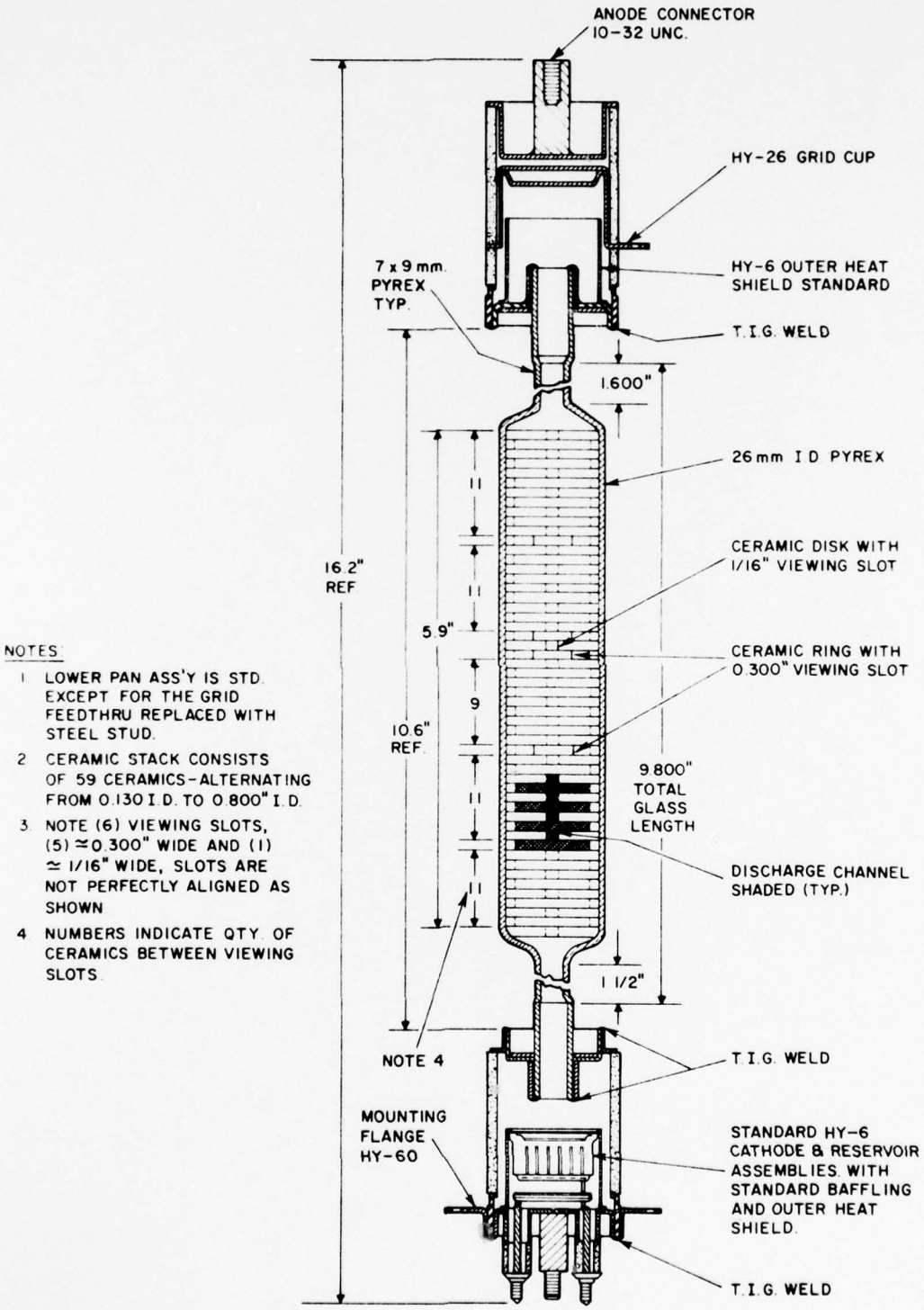

NOTES:

1. LOWER PAN ASS'Y IS STD. EXCEPT FOR THE GRID FEEDTHRU REPLACED WITH STEEL STUD.
2. CERAMIC STACK CONSISTS OF 59 CERAMICS-ALTERNATING FROM 0.130 I.D. TO 0.800" I.D.
3. NOTE (6) VIEWING SLOTS, (5) ≃ 0.300" WIDE AND (1) ≃ 1/16" WIDE, SLOTS ARE NOT PERFECTLY ALIGNED AS SHOWN
4. NUMBERS INDICATE QTY. OF CERAMICS BETWEEN VIEWING SLOTS.

Figure 3. RSI 005.

Table 1. Tube Design Specifications.

Tube No.	Internal Diameter (in.)	Interaction Tube Length (in.)	Fill Pressure (torr)	Fill Gas	Interaction Region Location
RSI 004	0.276	6 (magnet core limit)	0.400	H_2	Cathode-Grid Region
RSI 005	0.130	6 (straight discharge)	0.370	H_2	Cathode-Grid Region
	0.800	26 (maximum path length)			

2.2 OPTICAL SETUP FOR TUBE RSI 004

Two experimental arrangements used in the optical studies are shown in Figure 4. Since the $\vec{I} \times \vec{B}$ force on the plasma is perpendicular to the magnetic field, observation of the motion of the plasma during current interruption must be made in a direction parallel to the magnetic field. To do this, while retaining the tube position in the field, the arrangement shown in Figure 4a was used. In this configuration, the tube is subject to a non-homogeneous fringe field somewhat weaker than that within the core gap, and at an angle to the same. However, transverse plasma motion, although somewhat obscured, would still be expected to be visible. A reference grid was placed in front of the tube and a mirror was used to reflect the light path for the convenience of the experimental arrangement.

Spectroscopic measurements were made with direct tube observation, as shown in Figure 4b. Noise from firing the RSI and the magnet had an effect on experimental measurements, including a noticeable shift of the beam within the image converter tube. These errors were separated from the data presented in this report.

2.2.1 Image Converter Observations

An image converter containing a Mullard ME-1202 AA tube was obtained for optical use. The image converter trigger circuit is shown in Figure 5. An adjustable pulse width PFN is discharged by a KN-6B krytron through a transformer to provide an enabling 6-kV pulse to the image converter grid. The krytron is triggered from a second delay unit, after the magnet time delay, so that the image converter is gated for observations of short periods of the RSI discharge interruption time.

It was observed, with the RSI 004, that the plasma discharge narrowed and was directed toward one side of the discharge channel during application of the magnetic field. Examination of field directions indicated that the

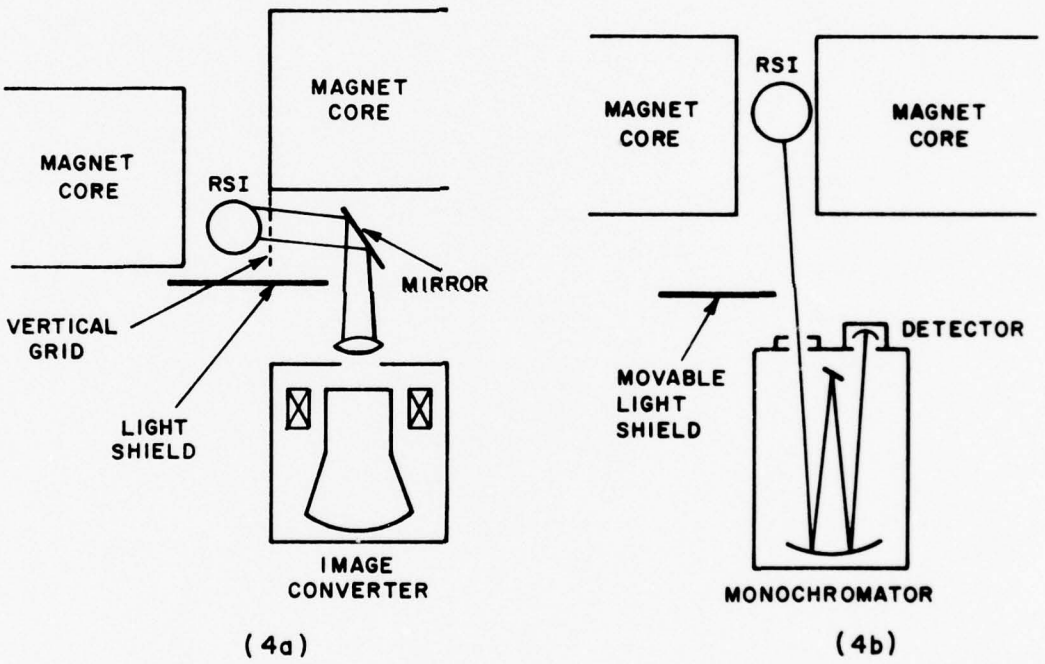

Figure 4. Optical Arrangement for Observing RSI 004.

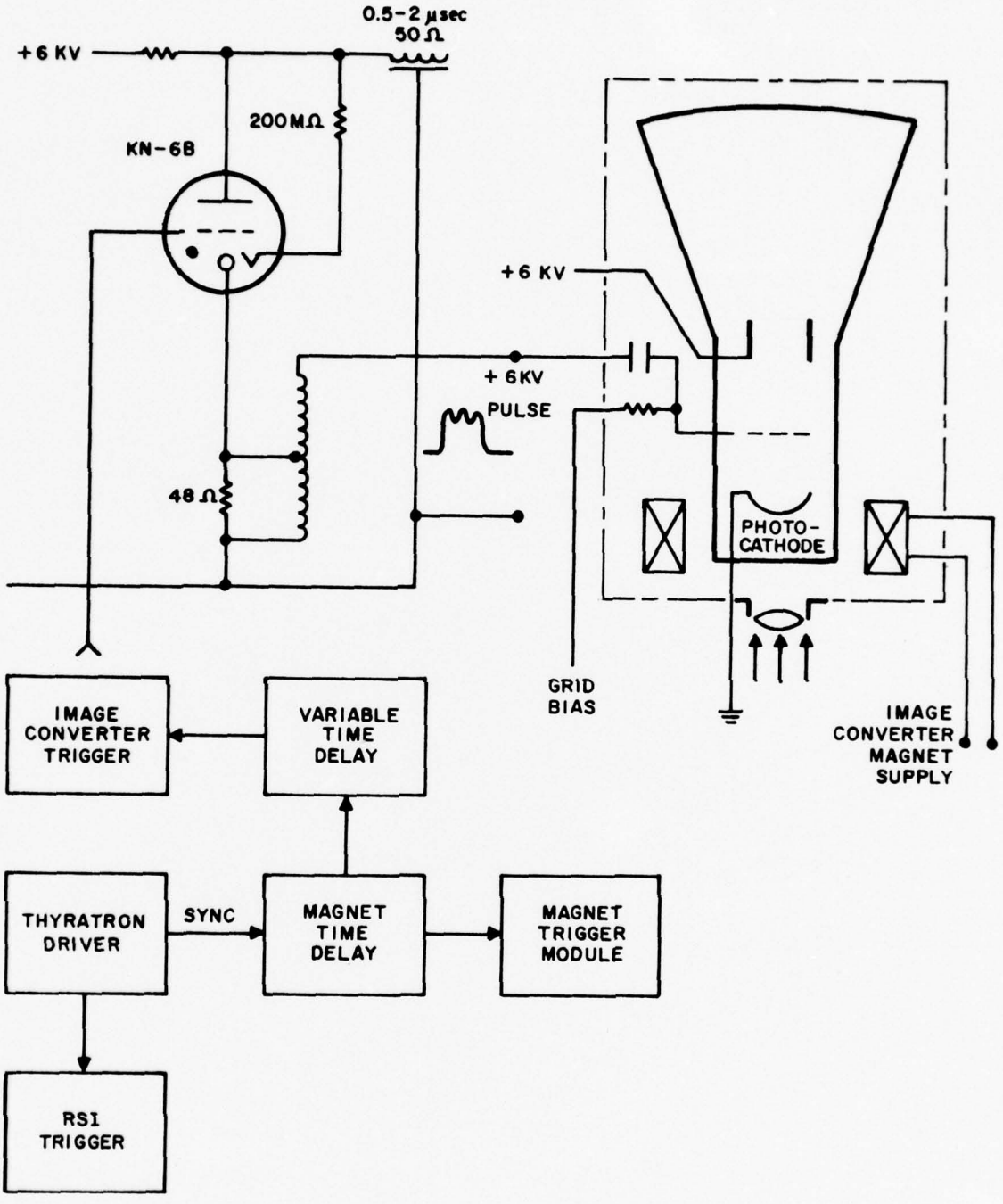

Figure 5. Image Converter Trigger Circuit.

plasma acted as it should for $\vec{I} \times \vec{B}$ behavior. Figure 6 shows some examples of the motion of the plasma column, where the light intensity is seen to follow the boundary of the interaction tube wall. The sketches are made directly from photographic observations.

Other photographs showed that as the discharge was interrupted, the plasma column became progressively narrower as a function of time. As would be expected, the light output from the tube diminished to nothing at nearly the same time (within experimental error) that the tube current went to zero.

When the applied magnetic field was slightly less than the interrupting field, it was observed, at high Ebb, that a relatively sudden change to a straight, intense, constricted discharge occurred 1 microsecond or so after the peak of the magnetic field. It is not apparent whether this represents a transition from glow to arc mode or whether it is a phenomenon associated with field constriction. Reduction of plasma channel diameter, by the application of a transverse magnetic field, is a real possibility being explored theoretically at present. Other studies show that a positive column contraction can be determined to be a result of high plasma temperature gradients, density gradients, a shortage of high speed electrons, or the presence of electronegative gaseous impurities (in this case, oxygen). All these factors are present in the RSI 004, and may play a part in the observed constriction.

Further attempts were made to study the more short-lived behavior of the plasma column, by the use of a shorter image converter enabling pulses of 1 and 0.25 microsecond duration. No evidence of any unusual short-time plasma behavior was seen from these photographs. The 0.25 microsecond pulse width represented the limit of useful image converter operation.

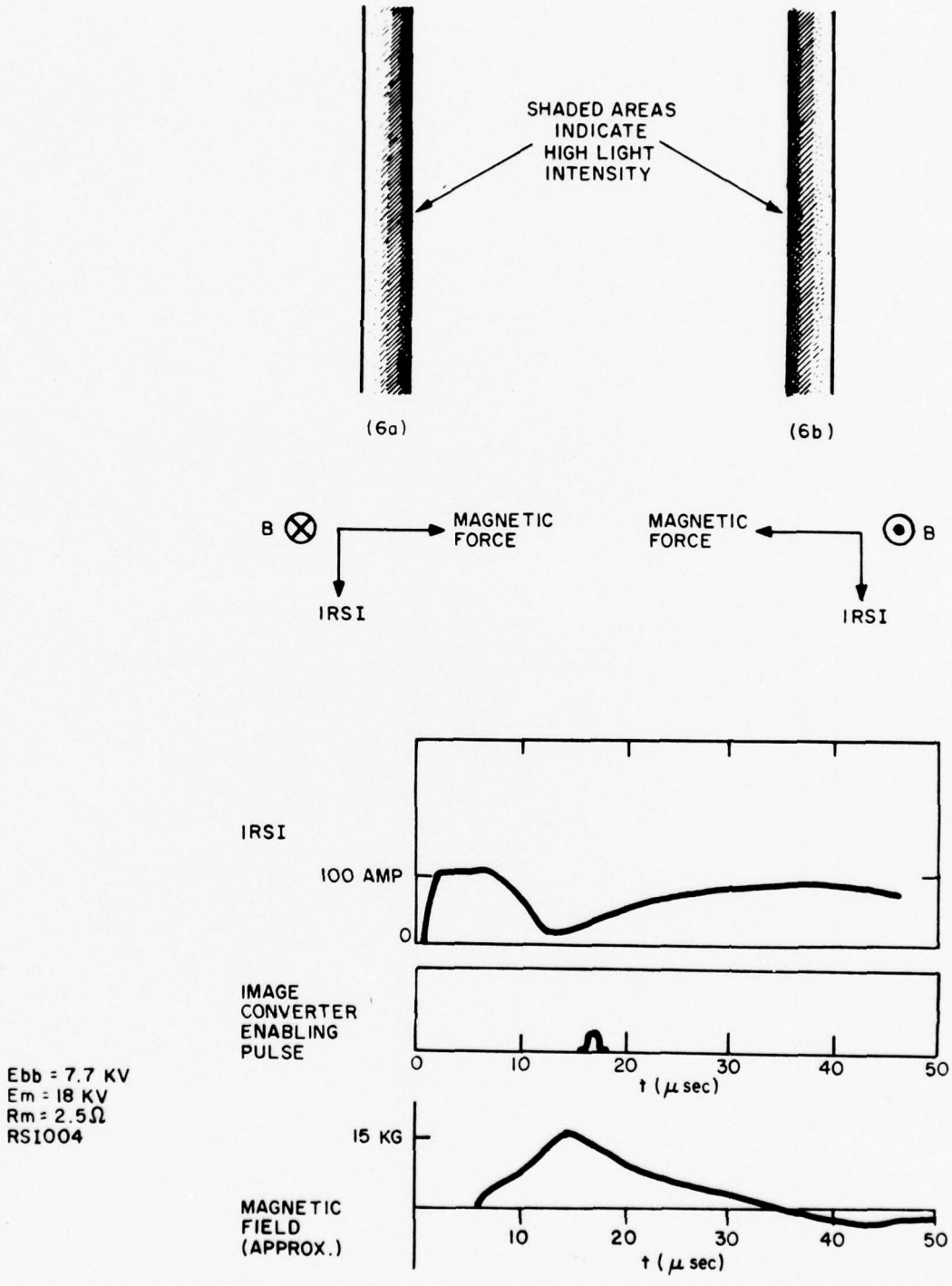

Figure 6. RSI 004 Light Intensity and Current and Magnetic Field Waveforms During Magnetic Field Interaction.

2.2.2 Spectrometer Studies

Two spectrometer systems used during this period were an EG&G Model 585 Spectroradiometer System, with a 10-nanometer bandpass monochromator, and a Jarrell-Ash 0.5-meter Ebert Scanning Monochromator. These were used in conjunction with EG&G detector heads or with an S-1 photomultiplier tube. Two, somewhat different, modes of operation were used: for the high intensity hydrogen and impurity wavelengths, the voltage from the photomultiplier was observed directly on an oscilloscope; for weak lines, the photomultiplier was linked to a long RC constant integrating circuit, which resulted in information concerning relative line intensities, but little information concerning the actual shape of the waveform.

Pronounced line wavelengths observed in this study were identified as: (1) members of the hydrogen Balmer series ($H\alpha$, $H\beta$, $H\gamma$, and $H\delta$); (2) the sodium 589.0, 589.6 doublet; (3) the 777.1, 777.4, 777.5 nm oxygen triplet; (4) many lines of the molecular hydrogen spectrum; and (5) impurity lines. The latter two categories evidenced only weak wavelength intensities. The sodium and oxygen were presumed to arise from components of the pyrex interaction tube wall.

The bulk of the light intensity from the RSI tube is, as expected, from the hydrogen lines, in the order of $H\alpha$, $H\beta$, and $H\gamma$. Figure 7 illustrates some of the waveforms of hydrogen for the RSI 004 (with different time scales). Figure 7a shows the short-term waveform during interruption and near interruption of the fault discharge. The output light intensity is seen to diminish to zero near the time that the discharge is interrupted – the delay shown may or may not be the real plasma deionization delay. It is significant to note the near doubling of light output from the discharge during the period in which the magnetic field is applied. Figures 7b and 7c show longer time scales of similar tests. The ringing seen in Figure 7b is due to ringing of the magnetic

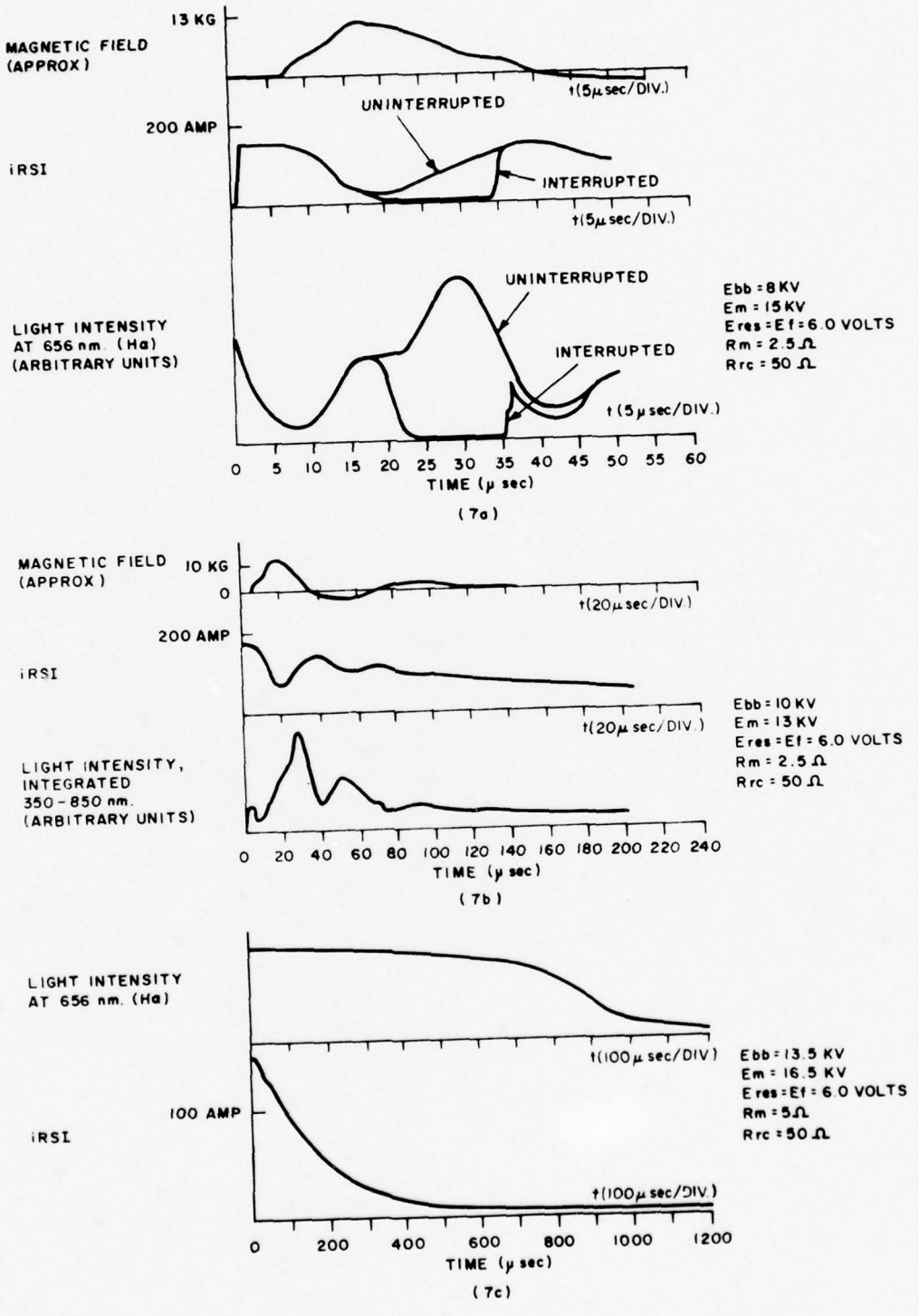

Figure 7. Hydrogen Light Intensity During Fault Conduction - RSI 004.

field (caused by small Rm for a high peak field). The ringing of the light intensity and the negative of the tube current follow the general shape of the applied magnetic field. Figure 7b reflects the total light output from the RSI (without the use of a monochromator).

Figure 7c shows the light intensity of the discharge over the entire period of the fault pulse. The intensity is nearly uniform for the body of the pulse, despite declining tube current.

Figure 8 shows the waveforms of light output for the sodium and oxygen lines. Both the sodium and oxygen lines first appear after application of the magnetic field. The sodium lines persist considerably longer than the oxygen lines, which appear to diminish to zero shortly after ringing of the magnetic field ceases. These lines arise from neutral sodium and oxygen atoms, which suggests that wall heating may cause the presence of the sodium line. Oxygen contamination of the plasma is a possibility, although decay of the oxygen line intensity during the fault pulse suggests otherwise.

Another test showed that the intensities of the sodium and oxygen lines were stronger by factors of 150 and 15, respectively, when the quenching field was applied (compared with a zero field condition), while the intensity of the major hydrogen lines integrated over the entire pulse changed relatively little. It could be concluded that the plasma-wall interaction is responsible for the introduction of the sodium and oxygen lines to the light output from the plasma.

Weaker lines were observed with the Jarrel-Ash monochromator, many of which were attributable to the complex molecular hydrogen spectrum. A 345.3-nanometer line was also seen, which is likely due to cobalt (345.4) which arises from the Kovar alloy (17.5% cobalt) used to seal the ends of the glass interaction tube. Visual examination of the tube after operation showed that this seal did undergo some slight melting at the point of plasma interaction.

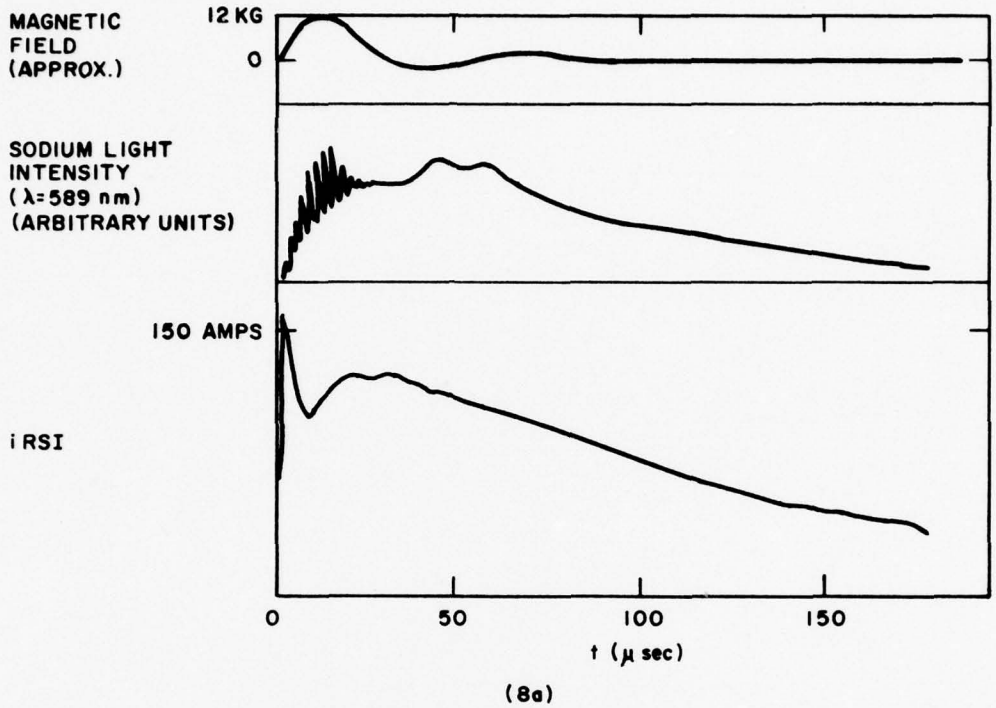

(8a)

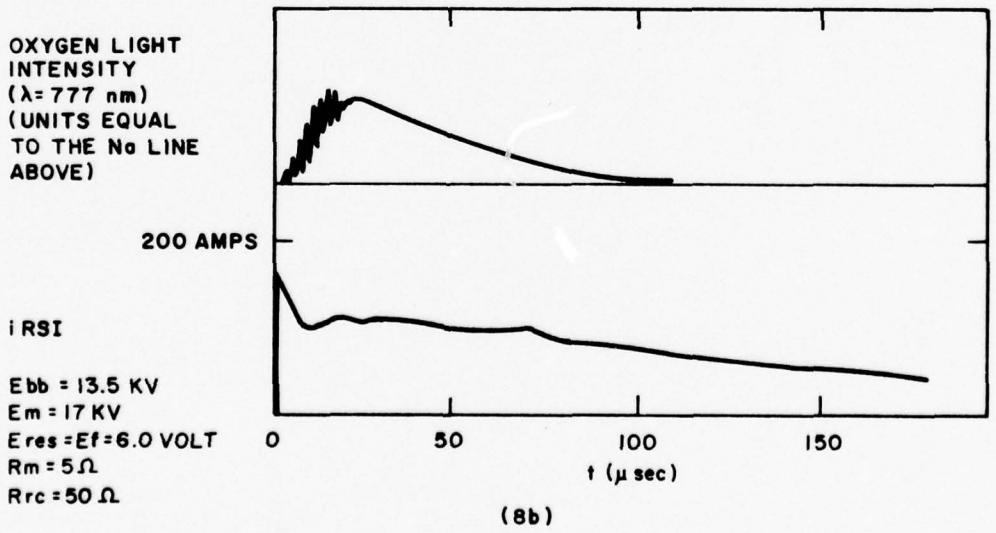

(8b)

Figure 8. Sodium and Oxygen Light Intensities During Fault Conduction - RSI 004.

2.2.3 Interaction Wall Damage

After considerable testing, the RSI 004 was removed from the magnet core. The tube was severely etched along a line down the length of the interaction tube wall, where the plasma had been driven against the wall. The etching followed a straight path about 2 mm wide, along the tube wall, expanding slightly to about 3 mm at the point of junction to the Kovar seals, where a slight change in tube internal diameter occurs.

During testing, the RSI 004 was rotated about its long axis and operated briefly with the plasma discharge striking a fresh wall surface. From this test it appears that surface degradation first occurs near the Kovar seals. The fact that it is at this point that the plasma first enters the magnetic field region may contribute to this behavior.

2.2.4 Electrical Measurements - RSI 004

Voltage drop measurements were taken for the RSI 004 at Ebb = 10 kV, prr = 300 pps, indicating a range of tube drop from 410 volts at Eres = 5.6 volts to 430 volts at Eres = 7.4. Allowing for a 100-volt drop in the cathode body and to the anode, this drop is roughly 14 volt/cm in the interaction tube. The improvement of voltage drop with pressure is not as pronounced for this tube as it had been for previous tubes, although the median value is about the same.

Magnetic field interrupting levels are shown in Figure 9, and are seen to be comparable with the interrupting field requirement observed for the single section RSI 003. The slight difference between the curves is probably due to the fact that the RSI 003 was tested at a lower pressure. Quenching values for both cases are, again, given in terms of a 50% probability of current interruption.

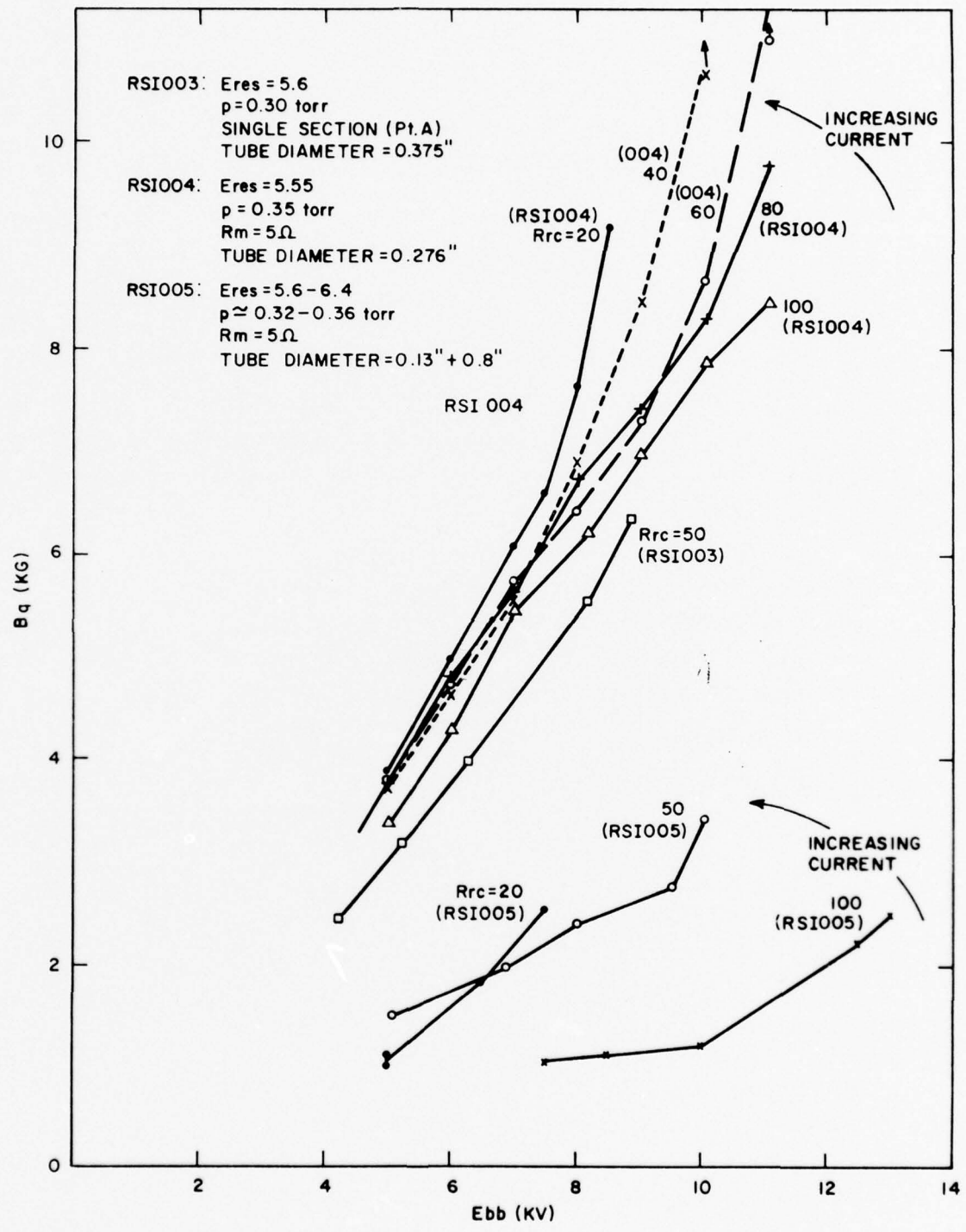

Figure 9. Interrupting Magnetic Field Versus Fault Pulse Current and Voltage.

2.3 RSI 005 STUDIES

Tube RSI 005 had a major problem in operation: during attempts to extinguish the fault discharge at moderate Ebb, the tube arced in the thin volume between the ceramic washers and the glass wall. This arcing occurred in the direction in which the plasma column was magnetically propelled, and was observed to occur in the same pulse that a glow discharge continued in the central discharge channel of the tube. After further studies, an attempt will be made to shrink the glass onto the surface of the ceramic washers, to eliminate the gap in which the arcing occurred.

Despite the arcing problem, useful results were obtained for the tube, with interrupting field requirements as shown in Figure 9. Present interrupting fields were compared with the field levels required for RSI 003 and RSI 004 interruption, and it is observed that the required field has been reduced to a factor of 30 - 50% of the straight discharge column tubes. Since this occurs even while the tube occasionally runs in the arc mode, avoiding the ceramic washer "plasma chute" section, it is probable that these improvements will increase when subsequent tubes operate properly.

If the interrupting field requirement were expected to obey the $Bq \alpha L^{-0.7}$ relationship determined from the RSI 003 tube, and if L, the interaction tube length, can be taken in this case as the path length of a discharge along a folded internal wall, then the relationship:

$$\frac{\text{Bq (folded wall tube)}}{\text{Bq (straight tube)}} \approx \left(\frac{26 \text{ in.}}{6 \text{ in.}} \right)^{-0.7} \approx 0.36$$

would be expected to hold. This factor is in general agreement with our observed results, but may not necessarily explain the tube behavior, since the mean free electron paths and the electron cyclotron radius are of the same general dimension as the washer-to-washer gap.

RSI 005 voltage drop was measured to range from 500 to 550 volts without a clear trend as a function of pressure. Allowing for voltage drops in the cathode, anode, and straight sections of the plasma cavity, the voltage drop in the washer section of the tube is approximately 16 volts/cm, which is only slightly more than that observed in the RSI 004. This is better than might be expected, since another study (Reference 1) showed that a bellows-like discharge channel could increase the voltage drop as compared to a straight channel, with the internal diameter equal to the central bore of the bellows.

It was seen in normal operation that, although a glow appeared in the washer-to-washer gap, the principal discharge followed a path with a diameter equal to the 0.130-inch diameter of the bore of the large constricting washers.

2.4 RESERVOIR AND FILAMENT HEATER SEPARATION

In previous work, pressure studies were performed by varying the RSI heaters with a single Variac control. In order to allow for testing RSI tubes at low pressure with a hot cathode, separate controls were introduced. Figure 10 and the lower curves of Figure 13 show the variation of interrupting fields with respect to different reservoir and filament heater voltages. The 10-15% change, caused by the adjustment of the filament heater, compares with the expected change in pressure of roughly that percentage due to parasitic heating of the reservoir by the cathode filament heater.

These data agree with previous results, showing a decrease in the magnetic field for interruption with a decrease in tube pressure.

2.5 MAGNETIC FIELD EXAMINATION

To ascertain the exact levels of magnetic field in this experiment, a magnetic field testing coil and circuit were designed, as shown in Figure 11a. Previously, a Hall effect gaussmeter had been tested but gave unusable results, presumably because of the fast rise time of our magnetic field pulse.

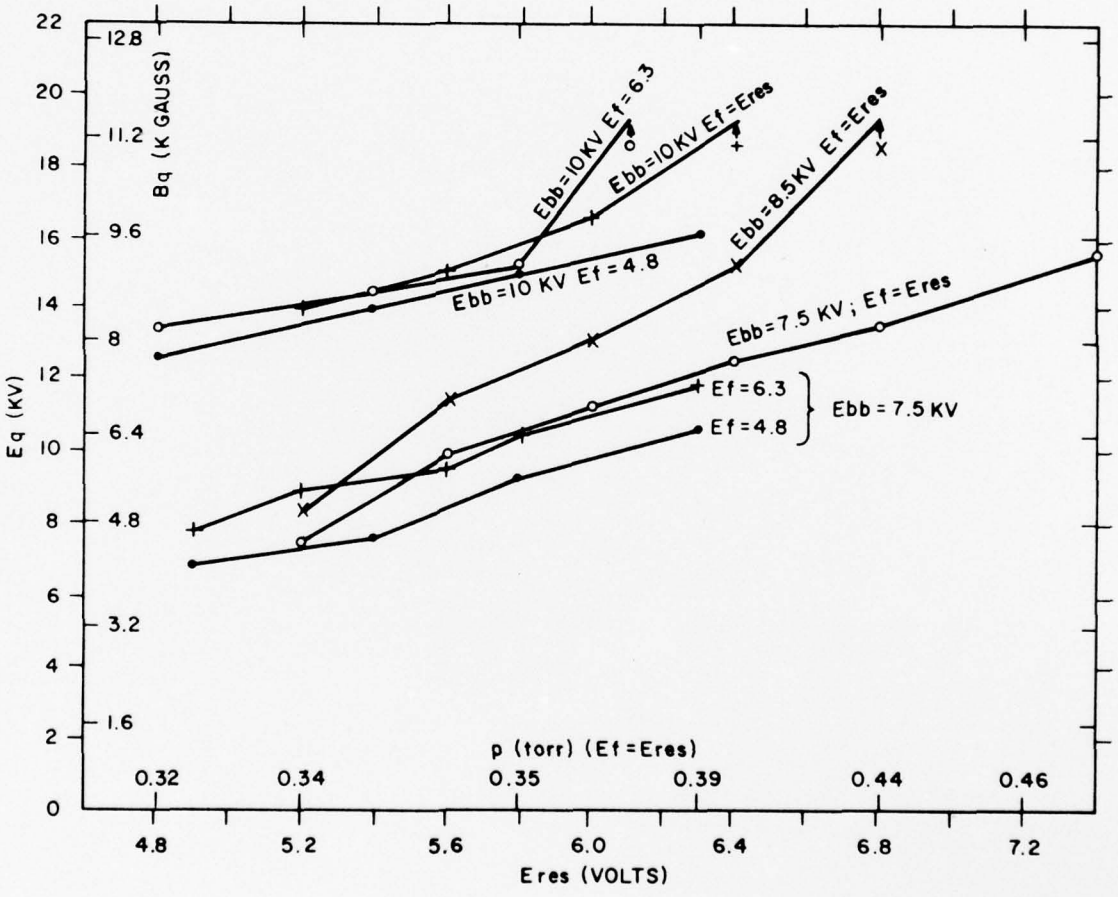

Figure 10. Interrupting Magnetic Field versus Tube Pressure for RSI 004.

The equation governing the pickup coil derives from:

$$\oint E \cdot d\ell = -\frac{300}{c} \int_S \dot{B} \cdot \vec{n} dA \text{ (volts, gauss, cm, sec)}$$

For our coil:

$$V_s = N \oint E \cdot d\ell \cong -\frac{300N}{c} \frac{\partial B}{\partial t} \pi r^2$$

where N = number of turns in the coil, and r = coil radius.
The circuit equation for Figure 11a is:

$$V_s = (L_1 + Lcoil)\, \dot{I}_p + (Rchoke + Rcct)\, I_p$$

where a choke has been added to the circuit for integration of the signal.
Combining equations, we find:

$$B = -\frac{c}{300N\, \pi r^2} \left\{ (L_1 + Lcoil)\, I_p + (Rchoke + Rcct) \int I_p dt \right\}$$

or:

$$B \cong -\frac{c}{300N\, \pi r^2} (L_1 + Lcoil)\, I_p$$

The test circuit was designed to minimize Rcct, and the choke was selected for minimal Rchoke, so that the peak field was nearly proportional to the peak circuit current. This current, measured by a current transformer, and corrected for the resistive error, accurately followed the waveform of the magnet current pulse, as shown in Figure 11b. The negative current for I_p at $t > 50$ μsec is a result of the resistive error above, and does not represent a change in magnetic field direction.

With this coil, an examination was made of the field distribution in our magnetic core gap, with results as shown in Figure 12. Peak field calculations for these fields and for the magnet under a variety of different gaps and magnet currents were calculated and compared with those predicted from

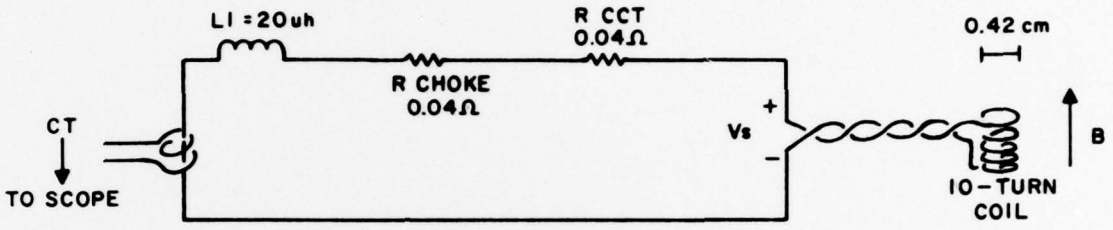

(11a)

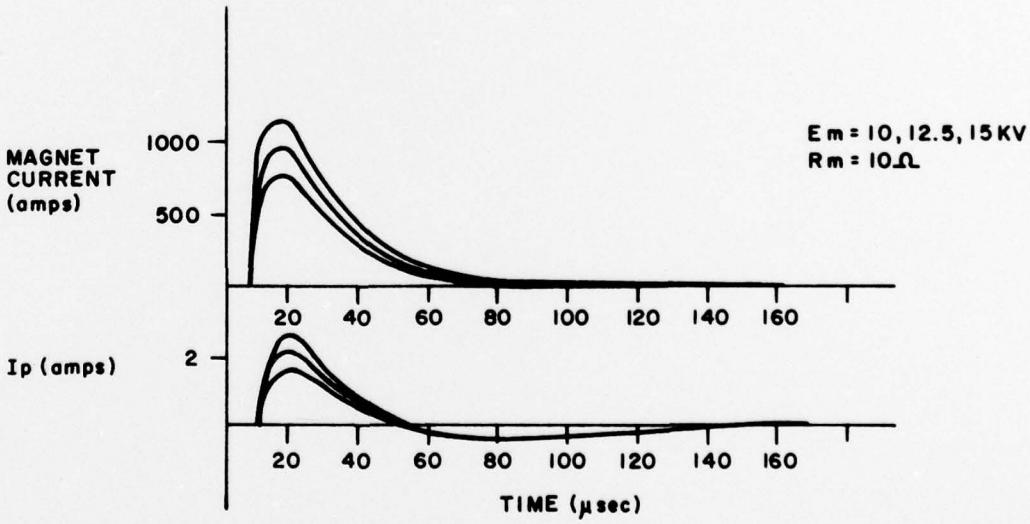

(11b)

Figure 11. Magnetic Field Testing Circuit and Output Waveform.

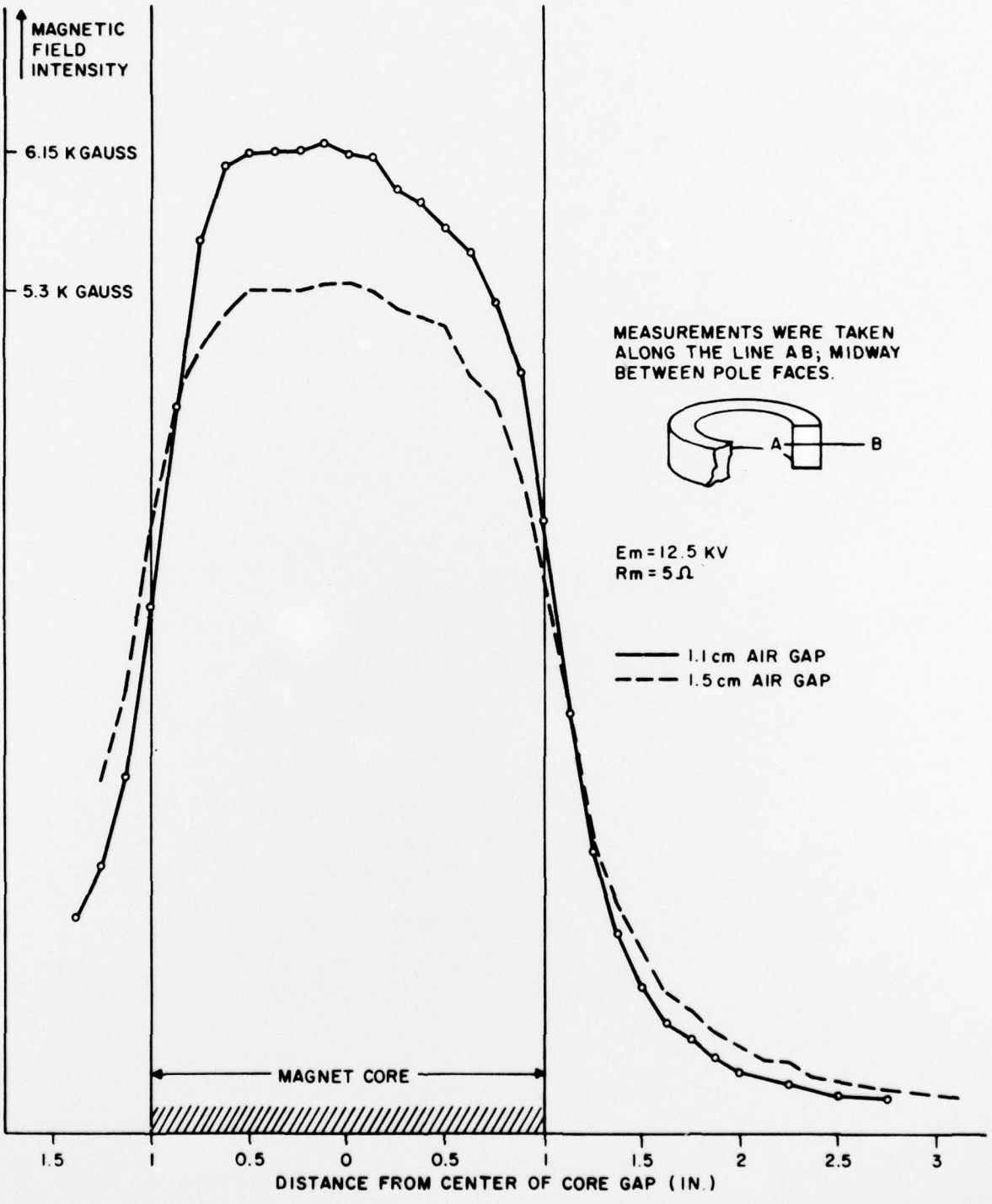

Figure 12. Magnetic Field Intensity versus Position within the Air Gap.

former field calculations, with the result that our experimental values ranged from 77 to 83% of our previous "theoretical" values. Field values given in previous reports should, therefore, be reduced by 20% of their value for accuracy. Values used in this report have already been corrected.

2.6 MAGNET FIRING DELAY STUDY

In connection with the reservoir-cathode study previously mentioned, a second examination of the effects of magnet firing delay on quenching requirements was undertaken with the RSI 004. The results are shown in Figure 13. It is noted that previous results (Second Triannual Report), indicating a reduction of interrupting field at low time delays, are not duplicated here. Instead, lower time delays increase quenching field levels, as long as the fault current has reached, and somewhat stabilized itself, at its maximum value. Changing the magnetic field rise time, by changing the number of turns (N) on the magnet core, did not change this behavior.

A possible cause of this change in behavior is the shorter interaction length in use. The previous study was done with the full RSI 003 interaction tube of 32 inches, as compared with the effective 6-inch tube in present use. The long, folded-type of discharge tube may require a longer time for full plasma generation. Since we expect to utilize a short interaction main length in our final design, we cannot expect to improve our quenching field requirements by timing effects unless we are able to trigger the magnet before the fault current has reached and stabilized at its maximum level.

The "error bar" range of values shown in the lower curves of Figure 13 represents the transition from quenching 50% of the fault pulses (lower points) and interrupting roughly 90% of the fault pulses (upper points).

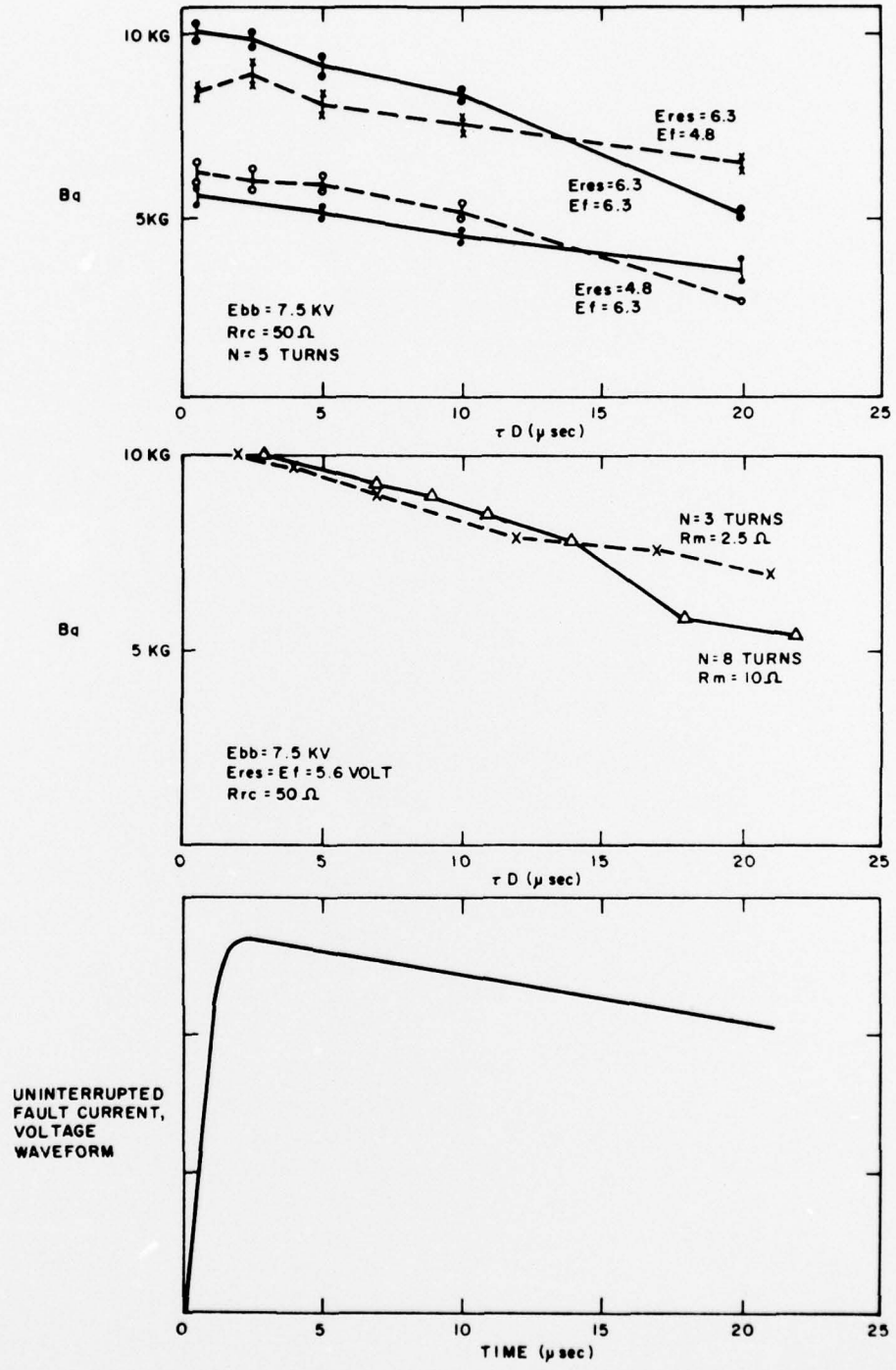

Figure 13. Interrupting Field versus Magnet Firing Delay Time - RSI 004.

2.7 EXPERIMENTAL MODIFICATIONS

A number of test changes have already been discussed. In addition, changes were made in the magnet coil circuit for the investigation of magnetic field requirements for holding off the fault current once interrupted. The magnetic field coil was replaced with a 10-turn coil, with current taps, for altering the number of turns in use. An additional magnet capacitor was added to the circuit for additional magnet current capability, and for alteration of the magnet current pulse shape. Preliminary tests on this circuit indicate that application of the magnetic field to the anode-grid holdoff region may substantially effect the prevention of restriking the fault current after interruption.

3. CONCLUSIONS

The optical evidence presented herein confirms the belief that the plasma column is moved bodily by the magnetic field against the interaction channel wall. Image converter observations and interaction channel damage observation indicate a narrowing of the discharge column during magnetic field interaction, and suggest that the plasma column in a transverse field assumes a separate, distinct physical mode with a well-defined, but constricted, discharge column diameter. Photographic evidence appears to reveal a transition from a normal glow to a shifted glow and, if circumstances allow, to a dense constricted discharge mode, within the 10-microsecond time scale of the magnetic field rise time. Experimentation with longer, more uniform magnetic field pulses might yield further information concerning the latter of these behaviors, but would have only indirect application to RSI development, insofar as current interruption must necessarily occur during a transitional time period of rising magnetic field strength. Long time scale plasma constriction, therefore, while of physical interest, is not being currently explored.

Use of a quenching transverse magnetic field therefore implies that interaction channel geometries must be constructed to allow for maximum plasma-wall interaction. The "plasma chute" design of RSI 005 strongly suggests that such geometries can effectively reduce the required magnetic quenching field, but normal behavior in these designs must be explored more closely. Tube jitter, high for RSI 005, must be reducible, most probably by an established keep-alive in the interaction channel. Tube voltage drop numbers appear to be reasonable.

Current work again indicates the preference of low tube pressure. Slight modification in final tube design (anode-grid spacing, cathode size) may be made to accommodate operation at a moderately lower pressure.

4. CONTINUING STUDIES

Our principal objectives at present are to direct the RSI program toward: (1) the interruption of fault currents at higher voltages, and (2) the optimization of the magnetic field pulse shape for effective and reliable current interruption and subsequent high voltage holdoff. These, and the continuing problems of tube voltage drop, magnetic field energy requirement, tube triggering, and lifetime must be considered in the design of new experimental tubes and circuitry. New methods of devising plasma chute-type tubes are being explored, and accommodations of our present experiment to higher voltages are underway.

4.1 TUBES UNDER DESIGN

RSI 006

This tube is a six section maze similar to RSI 003, but with an internal diameter of 0.25 inch. A narrow diameter anode-grid section will be appended to the tube for examination of the effects of a magnetic field across this region of the thyratron.

RSI 007

This tube will be composed of a variable anode-grid spacing section appended to a normal thyratron body for the investigation of holdoff capabilities of small diameter anode-grid regions. It is intended that this tube complement RSI 006 in this regard.

RSI 008

This tube will be built for the purpose of better delineating the effect that tube diameter has upon interaction channel voltage drop. The body of this tube will be constructed of impervious machinable ceramic with a series of differing diameter channels drilled through the ceramic, each with connecting access to a single main thyratron cathode section below.

RSI 009, RSI 010

These tubes are revisions of RSI 005 for studying the use of arc chutes on magnetic fault interruption. Machinable ceramic will again be used, with intersecting channels providing the chute-type design. Differing channel diameters, lengths, and spacings will be studied.

4.2 *OTHER STUDIES*

As previously mentioned, investigations concerning the effect of the shape of the magnet current pulse are being started. A compound pulse composed of a short, strong shut-off pulse and a long, weak hold-off pulse will be explored, as well as a variety of single pulses of differing duration.

The Machlett triode must yet be placed in the circuit for RSI testing. This should be done for testing the RSI 006 and subsequent tubes. Also in coordination with the RSI 006, a Langmuir probe setup is being designed.

Theoretical work is beginning in an attempt to identify the actual cause of the magnetic-induced increase in tube voltage drop. One possible mechanism involves consideration of the magnetic field as a means of narrowing the effective discharge channel, and thereby increasing the tube drop.

A life test will be arranged for the RSI 001. The unusual operating conditions of the RSI tubes require some modifications to the normal equipment for thyratron life testing.

Concern is being given to increasing the voltage capability of our experimental setup, with regard given to doubling Ebb.

5. REFERENCES

1. Robinson, T. S. et al. 1970. "Current Limitation and Pressure Gradients in the Non-uniform Long Positive Column," Journal of Physics D: Applied Physics (Great Britain), Vol. 3, p. 69.

DISTRIBUTION LIST

12 Defense Documentation Center
ATTN: DDC-TCA
Cameron Station (Bldg 5)
Alexandria, VA 22314

1 Code R123, Tech Library
DCA Defense Comm Engrg Ctr
1860 Wiehle Ave
Reston, VA 22090

1 Defense Communications Agency
Technical Library Center
Code 205 (P.A. TOLOVI)
Washington, DC 20305

1 Office of Naval Research
Code 427
Arlington, VA 22217

1 Director
Naval Research Laboratory
ATTN: Code 2627
Washington, DC 20375

1 Commander
Naval Electronics Laboratory Center
ATTN: Library
San Diego, CA 92152

1 CDR, Naval Surface Weapons Center
White Oak Laboratory
ATTN: Library, Code WX-21
Silver Spring, MD 20910

1 Rome Air Development Center
ATTN: Documents Library (TILD)
Griffiss AFB, NY 13441

1 Hq, Air Force Systems Command
ATTN: DLCA
Andrews AFB
Washington, DC 20331

2 CDR, US Army Missile Command
Redstone Scientific Info Center
ATTN: Chief, Document Section
Redstone Arsenal, AL 35809

1 Commander
US Army Missile Command
ATTN: DRSMI-RE (Mr. Pittman)
Redstone Arsenal, AL 35809

3 Commandant
US Army Aviation Center
ATTN: ATZQ-D-MA
Fort Rucker, AL 36362

1 Director, Ballistic Missile Defense
Advanced Technology Center
ATTN: ATC-R, PO BOX 1500
Huntsville, AL 35807

1 Commander
HQ Fort Huachuca
ATTN: Technical Reference Div
Fort Huachuca, AZ 85613

2 Commander
US Army Electronic Proving Ground
ATTN: STEEP-MT
Fort Huachuca, AZ 85613

1 Commander
USASA Test & Evaluation Center
ATTN: IAO-CDR-T
Fort Huachuca, AZ 85613

1 Deputy for Science & Technology
Office, Assist Sec Army (R&D)
Washington, DC 20310

1 CDR, Harry Diamond Laboratories
ATTN: Library
2800 Powder Mill Road
Adelphi, MD 20783

1 Director
US Army Ballistic Research Labs
ATTN: DRXBR-LB
Aberdeen Proving Ground, MD 21005

1 Harry Diamond Laboratories, Dept of Army
ATTN: DRXDO-RCB (Dr. J. Nemarich)
2800 Powder Mill Road
Adelphi, MD 20783

1 Commander
US Army Tank-Automotive Command
ATTN: DRDTA-RH
Warren, MI 48090

1 CDR, US Army Aviation Systems Command
ATTN: DRSAV-G
PO Box 209
St. Louis, MO 63166

1 TRI-TAC Office
ATTN: CSS (Dr. Pritchard)
Fort Monmouth, NJ 07703

1 CDR, US Army Research Office
ATTN: DRXRO-IP
PO Box 12211
Research Triangle Park, NC 27709

1 CDR, US Army Research Office
ATTN: DRXRO-PH (Dr. R. J. Lontz)
PO Box 12211
Research Triangle Park, NC 27709

1 Commandant
US Army Air Defense School
ATTN: ATSA-CD-MC
Fort Bliss, TX 79916

1 Commander, DARCOM
ATTN: DRCDE
5001 Eisenhower Ave
Alexandria, VA 22333

1 Naval Surface Weapons Center
Dahlgren Laboratory
ATTN: Dr. M. Rose, Code DF-102
Dahlgren, VA 22448

1 Ballistic Missile Defense Advanced Technology Center
ATTN: Dr. L. Havard, ATC-T
P.O. Box 1500
Huntsville, AL 35807

1 Air Force Aero Propulsion Laboratory
ATTN: Mr. R. Verga, AFAPL/POD-1
Wright Patterson Air Force Base
Ohio 45433

1 Chief
Ofc of Missile Electronic Warfare
Electronic Warfare Lab, ECOM
White Sands Missile Range, NM 88002

Commander
US Army Electronics Command
Fort Monmouth, NJ 07703
1 DRSEL-GG-TD
1 DRSEL-WL-D
3 DRSEL-CT-D
1 DRSEL-TL-DT
3 DRSEL-TL-BG
1 DRSEL-TL-BG (Ofc of Record)
2 DRSEL-MS-TI
1 DRSEL-TL-D
25 Originating Office

2 MIT - Lincoln Laboratory
ATTN: Library (RM A-082)
PO Box 73
Lexington, MA 02173

1 NASA Scientific & Tech Info Facility
Baltimore/Washington Intl Airport
PO Box 8757, MD 21240

2 Advisory Group on Electron Devices
201 Varick Street, 9th Floor
New York, NY 10014

1 ITT Electron Tube Division
3100 Charlotte Avenue
Easton, PA 18042